Shape study of the $N = Z$ nucleus ^{72}Kr via β decay

J. A. Briz,[1,*] E. Nácher,[1,2] M. J. G. Borge,[1,3] A. Algora,[2,4] B. Rubio,[2] Ph. Dessagne,[5,6] A. Maira,[1] D. Cano-Ott,[2,7] S. Courtin,[5,6] D. Escrig,[1] L. M. Fraile,[8] W. Gelletly,[9] A. Jungclaus,[1] G. Le Scornet,[3] F. Maréchal,[5,6] Ch. Miehé,[5,6] E. Poirier,[5,6] A. Poves,[10] P. Sarriguren,[1] J. L. Taín,[2] and O. Tengblad[1]

[1]*Instituto de Estructura de la Materia, CSIC, Serrano 113-bis, E-28006 Madrid, Spain*
[2]*Instituto de Física Corpuscular, CSIC - Universidad de Valencia, E-46071 Valencia, Spain*
[3]*ISOLDE-PH, CERN, CH-1211 Geneva 23, Switzerland*
[4]*Institute of Nuclear Research of the Hungarian Academy of Sciences, Debrecen H-4001, Hungary*
[5]*IPHC, Université de Strasbourg, F-67037 Strasbourg, France*
[6]*CNRS, UMR7178, F-67037 Strasbourg, France*
[7]*Centro de Investigaciones Energéticas, Medioambientales y Tecnológicas, E-28040, Madrid, Spain*
[8]*Grupo de Física Nuclear, Facultad de Físicas, Universidad Complutense - CEI Moncloa, E-28040 Madrid, Spain*
[9]*Department of Physics, University of Surrey, Guildford, GU2 5XH, United Kingdom*
[10]*Departamento de Física Teórica e IFT-UAM/CSIC, Universidad Autónoma de Madrid, Madrid, Spain*

(Received 3 September 2015; published 30 November 2015)

The β decay of the $N = Z$ nucleus ^{72}Kr has been studied with the total absorption spectroscopy technique at ISOLDE (CERN). A total $B(\mathrm{GT}) = 0.79(4) g_A^2/4\pi$ has been found up to an excitation energy of 2.7 MeV. The B(GT) distribution obtained is compared with predictions from state-of-the-art theoretical calculations to learn about the ground state deformation of ^{72}Kr. Although a dominant oblate deformation is suggested by direct comparison with quasiparticle random phase approximation (QRPA) calculations, beyond-mean-field and shell-model calculations favor a large oblate-prolate mixing in the ground state.

DOI: 10.1103/PhysRevC.92.054326 PACS number(s): 23.40.Hc, 29.30.Kv, 27.50.+e, 21.10.Pc

I. INTRODUCTION

The study of the structure of neutron-deficient atomic nuclei with A $\approx$ 70–80 is particularly challenging for both experiment and theory. One of the reasons is that shape transitions and shape coexistence phenomena are expected to occur in these nuclei [1,2]. The Nilsson model [1,3] shows large energy gaps in the energy versus quadrupole deformation diagram at $Z, N = 34$, 36, and 38 for oblate and prolate deformations. The single particle level gap at $N = 38$ is responsible for the large prolate deformation observed for the $N = Z = 38$ nucleus ^{76}Sr [4,5]. However, the gap found at $Z, N = 36$ for oblate deformation competes with this, leading to several energy minima close in energy (<2 MeV) in the potential energy surface [6,7]. This is the reason for the shape coexistence already observed in ^{72}Se [8] and ^{74,76}Kr [9]. The experimental signatures for this phenomenon are the observation of low-lying 0^+ states, which are interpreted as the bandheads of states of different shapes, and $E0$ transitions between them.

The theoretical work of Möller *et al.* [7] presented ^{72}Kr as a clear example of nuclear shape coexistence due to the occurrence of three energy minima corresponding to oblate, prolate, and spherical shapes within an energy interval of around 1.4 MeV. The first evidence for shape coexistence in this nucleus came from the similarity of the in-beam ^{72}Kr and ^{72}Se γ spectra observed in studies of ^{72}Kr produced in heavy-ion-induced fusion-evaporation reactions [10]. The 0_1^+ ground state of ^{72}Kr is predicted to have an oblate deformed shape in different theoretical approaches [1,2,7]. The 0_2^+ state was observed at an excitation energy of $E = 671(2)$ keV and interpreted as the prolate bandhead [11]. Assuming a simple two-level scheme for these two 0^+ states, it was found that a mixing ratio of $\lambda = 0.1$ is needed to account for their relative energies. There, the unperturbed energies of the two 0^+ states were estimated from extrapolation of the rotational states towards lower spins.

A prolate high-spin band was reported from the 4^+ state ($E = 1322$ keV) upwards in Ref. [12]. The authors predicted a prolate-oblate shape transition below this level. The transition strength $B(E2; 0_1^+ \rightarrow 2_1^+)$ value was measured by A. Gade *et al.* [13] in an intermediate energy Coulomb excitation experiment providing a value of 4997(647) e^2 fm^4. It corresponds to a quadrupole deformation parameter $|\beta_2| = 0.33(2)$. A recent determination of the strengths of the deexciting transitions from the 4^+ state [14] provided a value $B(\mathrm{E2}; 4_1^+ \rightarrow 2_1^+) = 2720(550)$ e^2 fm^4, which suggests that the 2_1^+ state is prolate. Meanwhile the reduced value of the $B(\mathrm{E2}; 2_1^+ \rightarrow 0_1^+) = 810(150)$ e^2 fm^4 [14] reinforces the idea of a shape transition to an oblate 0_1^+ ground state or shape mixing between these two low-lying 0^+ states. The newer value of the $B(\mathrm{E2}; 2_1^+ \rightarrow 0_1^+)$ agrees with the previous result of [13]. Preliminary results from a recent experiment on the Coulomb excitation of the ^{72}Kr ground state [15] also

*jose.briz@subatech.in2p3.fr; Current address: Subatech Lab., IN2P3-CNRS, École des Mines de Nantes and Univ. Nantes, 4 rue Alfred Kastler, La Chantrerie BP 20722, 44307 Nantes Cedex 3, France.

suggest that the 2_1^+ state is prolate. Despite the quite numerous experiments and results, no direct evidence for the sign of the deformation of the ^{72}Kr ground state has been found so far.

Here we used a different approach to study the deformation of ^{72}Kr. Instead of using nuclear reactions to reach excited states in ^{72}Kr and get information on its excited structure, we infer the deformation of its ground state from its β-decay properties. It is worth noting that, in contrast with previous experiments, this investigation concerns only the ground state. It was shown in the pioneering work of Hamamoto and Zhang [16] that the energy dependence of the reduced Gamow-Teller transition probability, namely the B(GT) distribution, for nuclei in the mass region A $\approx$ 70–80 depends sensitively on the nuclear shape. Following this idea, calculations using the quasiparticle random phase approximation (QRPA) approach [6] showed several energy minima in the potential energy surface close in excitation energy (shape coexistence). The calculated B(GT) distribution in the decay of each of these states corresponding to a defined deformation is remarkably different.

Consequently, the experimental determination of the B(GT) distribution can provide information on the deformation of these nuclei by direct comparison with the theoretical predictions. The method implies the use of the total absorption spectroscopy (TAS) technique [17] to determine the β feedings to the states in the daughter nucleus and infer the B(GT) distribution of the decay of interest. This technique overcomes the systematic errors that arise from the use of low-efficiency detectors, namely the "Pandemonium effect" introduced in [18], and offers the possibility to determine the B(GT) experimentally in a reliable manner.

Oblate deformed nuclei are scarce in the chart of nuclides. Any experimental evidence for them would be helpful to test the different theoretical approaches. This would contribute to our understanding of the mechanisms leading to shape transitions as well as the reason for the general dominance of prolate deformation. Thus, the study of those nuclei predicted to have an oblate deformed shape in their ground state, such as ^{70}Br or ^{72}Kr [1,2], is of great interest. The latter case is the subject of the present work thanks to the reasonably good yields available at the ISOLDE (CERN) facility.

The present work describes the β-decay study using the TAS technique for the $N = Z$ nucleus ^{72}Kr with the aim of shedding light on the deformation of its ground state. The resulting B(GT) distribution is compared with predictions from the best performing theoretical models in the mass region, namely the aforementioned QRPA calculations [6], beyond-mean-field calculations [19], and newly developed shell-model calculations. The *Lucrecia* TAS detection system permanently installed at the ISOLDE facility (CERN) was used. Previous studies on the shapes of nuclei in the mass region using this procedure and the same experimental setup have provided conclusive results for ^{76}Sr [4], ^{78}Sr [20] (both prolate), and ^{74}Kr [21] (shape mixing).

II. EXPERIMENT

The experiment was performed at the ISOLDE facility in CERN, Switzerland [22], where a 1.4 GeV proton beam

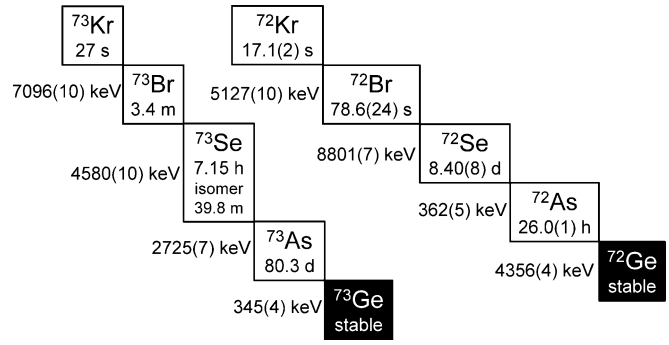

FIG. 1. $A = 73,72$ isobaric decay chains starting at ^{73,72}Kr. $T_{1/2}$ values are taken from [23] for $A = 72$ and [24] for $A = 73$ and the Q_{EC} values from [25].

of an intensity up to 2 μA impinged on a 43 g/cm^2 Nb target. The proton beam was pulsed following the CERN Proton Synchrotron Booster supercycle structure which, at the time of the experiment, consisted of 14 pulses containing $\approx 10^{13}$ protons each and spaced 1.2 s apart. Approximately half of these pulses were delivered to the ISOLDE facility. The reaction products were ionized using a plasma ion source connected to the target by a cold transfer line in order to suppress the transport of less volatile elements and reduce the isobaric contamination. Then, the ions were directed to the High-Resolution Separator (HRS), a system of two bending magnets providing a mass resolving power of $M/\Delta M = 5000$, where the $A = 72$ ions were further selected from all the remaining ionized elements coming from the ion source. The $A = 72$ ion beam, which consisted mainly of ^{72}Kr ions, was delivered to the total absorption spectroscopy experimental setup where it was collected on an aluminized mylar tape at the geometrical center of the TAS spectrometer. A system of three collimators with apertures of 36, 4, and 4 mm was employed to guarantee the deposition of beam ions exclusively on the mylar tape. A tape transport system was used to replace the sample periodically and remove the residual longer living activities in the isobaric decay chain. The duration of the measuring period was chosen according to the decay under study. For ^{72}Kr decay, the collection and measuring were simultaneous and lasted 15 seconds to maximize the amount of ^{72}Kr activity ($T_{1/2} = 17.1(2)$ s [23]) with respect to the daughter, ^{72}Br ($T_{1/2} = 78.6(24)$ s [23]). Fig. 1 shows the decay chains of ^{72,73}Kr.

A sketch of the experimental setup is shown in Fig. 2. The *Lucrecia* TAS spectrometer is a NaI(Tl) mono-crystal with a cylindrical shape of 38 cm base diameter and 38 cm height. The collection point was surrounded by ancillary detectors for particle identification and tagging: a high-purity germanium (HPGe) telescope detector composed of a 1-cm-thick planar and a 5-cm-thick coaxial detector covering approximately 14% of 4π for x- and γ-ray detection respectively and a 2-mm-thick plastic (NE102) scintillator for detecting β particles which covers around 13% of 4π. The light produced in the plastic was collected using two light guides connected to identical and independent photomultipliers. The signals from the β detector

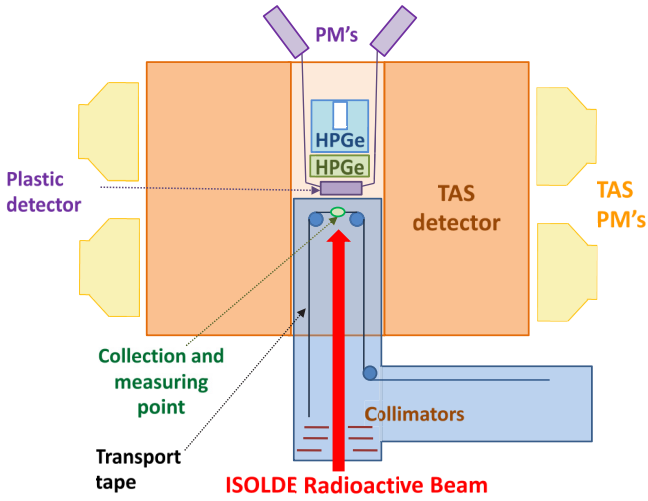

FIG. 2. (Color online) Horizontal cut of the experimental setup used in the β-decay study of ^{72}Kr. The *Lucrecia* total absorption spectrometer is a NaI(Tl) monocrystal which is complemented by ancillary detectors: a HPGe telescope for the detection of x and γ rays and a plastic detector for β particles. A tape transport system is used to periodically replace the sample. Eight large photomultipliers collected the scintillation light from the NaI(Tl) crystal and their analog signals were added.

were recorded only when the photomultipliers registered a signal simultaneously.

The data were acquired on a TAS-triggered event-by-event basis using a data acquisition system based on CAMAC-FERA electronics controlled by a VME processor. The measurement devoted to the ^{72}Kr decay was performed during 3.27 hours in three independent runs, and the counting rate was kept at low values ($\approx$3.5 kHz) to reduce the contribution of pile-up of electronic signals to the TAS spectrum.

III. ANALYSIS

The data analysis was performed following the procedure explained in detail in Refs. [26,27]. The experimental data, $d(i)$, are the result of the convolution of the β feeding distribution, $f(j)$, and the response of the detector to this distribution, $R(i,j)$. Mathematically, it can be expressed as

$$d(i) = \sum_j R(i,j) \otimes f(j). \quad (1)$$

The index i goes over all the spectrum divisions and j over the intervals in which one discretizes the de-excitation scheme of the daughter nucleus. Both intervals were chosen to be 40 keV wide. For the analysis, the response matrix of the detector to the decay of interest, $R(i,j)$, is needed. In order to calculate it we followed the procedure described in Ref. [28]. The response functions of the detector to the individual quanta, γ rays, and β particles, involved in the decay and also information on the daughter deexcitation scheme such as level energies and deexcitation branching ratios are required to determine the response matrix.

The response function of the *Lucrecia* TAS detector to monoenergetic γ rays and positrons was determined using GEANT4 simulations [29] of the experimental setup. The validation of the simulations was performed using several sources with well-known decay schemes such as ^{24,22}Na. The simulated spectra provided a satisfactory reproduction of the experimental results as described in Ref. [30].

The decay scheme of ^{72}Kr was divided into two regions: the so-called "known" part, where we assume that the information obtained in experiments carried out with high-resolution detectors (Ge) is complete, and the "unknown" part at higher energies where the level density is high and, as a result, the information from the high-resolution studies is incomplete. In the known part we use the level energies, spin-parities, and deexcitation branching ratios from the detailed high-resolution spectroscopy work of Piqueras *et al.* [31]. The conversion coefficients of the low-energy transitions are taken from the results obtained in a measurement carried out by our collaboration and partially presented in [32]. It is stated in Ref. [31] that the level scheme was complete in terms of the number of 1^+ states only up to $E = 1.173$ MeV, from a test of completeness performed by comparing the experimental number of 1^+ states with the mean accumulated level density obtained theoretically from the *constant temperature formula*. For this reason we make the conservative assumption that the "known" part extends up to $E = 1.0$ MeV.

The description of the unknown part follows the procedure described in detail in [27]. Levels are placed following the level density given by the back-shifted Fermi gas model [33] formula with parameters $a = 10.697$ MeV^{-1} and $\Delta = -0.839$ MeV. The level spacing is assumed to follow the Wigner distribution. The deexcitation branching ratios of the levels in the unknown part are obtained from γ-strength functions related to the nuclear giant resonance excitation modes by the Axel-Brink hypothesis [34]. Only transitions of $E1$, $M1$, and $E2$ multipolarity have been considered.

We built up the deexcitation branching ratio matrix using all this information on the excitation scheme of ^{72}Br. It describes how every excited level decays and the probability for each of the possible deexcitation paths. At this stage, we calculated the response matrix, $R(i,j)$, convoluting the deexcitation branching ratio matrix with the response function of the detector to the individual quanta involved in the decay. Reference [28] presents a more detailed description of this procedure.

The TAS data analysis involves an unfolding algorithm which employs the full statistics in the spectrum instead of the individual photopeaks considered in high-resolution spectroscopy. For this reason, it is extremely important to be sure that the spectrum contains only contributions from the decay of interest. Any other contribution with a different origin is undesired and will be referred to as a *contaminant*. Usually, the main sources of contamination in TAS spectra are the room background radiation, the decay of the descendants and the pile-up of electronic pulses in the analog-to-digital converter (ADC). The last of these components depends on the counting rate of the TAS during the measurement.

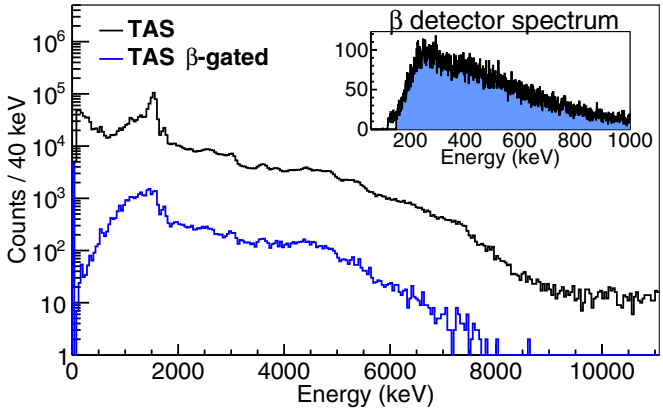

FIG. 3. (Color online) TAS spectra taken for ^{72}Kr decay during the first run of 75 min (black). The blue line shows the spectrum obtained when gating with a signal in the β detector using the coincidence energy window ($E > 150$ keV) shown in the top-right inset.

A. Contamination removal

The raw TAS spectrum shown in black in Fig. 3 reveals that some contaminants are present, since we observe counts in the spectrum beyond the $Q_{EC}(^{72}\text{Kr}) = 5127(10)$ keV value.

An inspection of the HPGe spectra confirmed that ^{72}Br and ^{72}As decay radiations were present; see Table I. Numerical estimates, based on the Bateman equations applied to the $A = 72$ isobaric chain starting at ^{72}Kr, see Fig. 1, were performed. They showed two disturbing effects: first, that the radioactive beam was contaminated with ^{72}As ions, and, second, that part of the beam was deposited outside the mylar tape. The ^{72}As activity found experimentally was much higher than that coming exclusively from the decay of the isobaric chain and it was growing continuously, as can be seen in the last column of Table I.

The ^{72}As contamination in the beam is understood as the ^{72}As ions passing through the cold transfer line in the form of a volatile dimer molecule (As_2). They are formed in cold environments but break when the environmental temperature grows, as happens at the exit of the cold transfer line. Then, the ^{72}As ions pass through the mass separator because they are close in mass to ^{72}Kr, and later reach the experimental setup mixed with the ^{72}Kr beam. Although the ^{72}As decay contamination is small in comparison with that of ^{72}Kr (see Table I) it could not be removed. For this reason, the analysis of the three runs available was performed independently instead of summing them and performing a single analysis. This allowed us to evaluate the influence of this contamination and its contribution to the errors.

TABLE I. Amount of isobaric nuclei present in each of the ^{72}Kr decay measurements obtained from the analysis of the HPGe telescope spectra. The most intense γ lines for each decay were used for this study: 415 keV from ^{72}Kr, 862 keV from ^{72}Br, and 834 keV from ^{72}As. Peak areas in the HPGe spectra taken in coincidence with a signal in the TAS spectrum are divided by detector efficiency and γ intensity per 100 parent decays.

	Duration (min)	Relative integrated activity		
		^{72}Kr	^{72}Br	^{72}As
^{72}Kr file 1	75	100(14)	8.2(14)	0.0
^{72}Kr file 2	74	100(13)	8.5(14)	1.5(2)
^{72}Kr file 3	47	100(13)	11.2(19)	2.4(4)

The background radiation was changing during the measurement due to the beam deposition outside the moving tape. This fact makes the analysis of the raw TAS spectrum unreliable. For this reason, we preferred to apply conditions to the TAS spectrum that obviate this problem. This can be done by selecting either the Electron Capture (EC) or β^+ components of the decay. In order to extract the EC component one can demand a coincidence with the daughter x rays in the HPGe detectors. For the case of ^{72}Kr this possibility was rejected because of the existence of several low-energy transitions in ^{72}Br with non-negligible conversion coefficients. This means that the x rays have two possible origins: the EC decay and the internal conversion. Therefore, the selection of the EC component was not guaranteed by this method. The other alternative is to study the β component since the β radiation from the decay of the ^{72}As deposited in the beam pipe could not reach the plastic detector. As a result, the β-gated spectrum could be obtained in a rather clean manner and, therefore, the β coincidence condition was chosen to perform the analysis. The electrons coming from converted transitions following the EC decay contribute to the β detector spectrum where we gate to choose the β^+-decay component. However, this contribution was estimated to be around 1.2% that of electrons from the β^+-decay branch of ^{72}Kr decay. This was later confirmed from our resulting feeding distribution.

Figure 3 shows the TAS raw spectrum (black) and the one obtained by demanding a coincidence in the TAS detector with a signal in the β detector, hereinafter called the β-gated spectrum (blue). An energy threshold of 150 keV was imposed to avoid electronic noise in the β spectrum. The condition removes the room background contamination completely. It reduces the statistics by a factor given by the efficiency of the plastic detector. One can observe in Fig. 3 that the β-gated spectrum extends beyond the Q_{EC} value of ^{72}Kr, 5127(10) keV, and corresponds to the decay of the daughter activity ^{72}Br, 8801(7) keV. Another relevant feature is the high statistics found in the energy region between 1.3 and 1.6 MeV which is in agreement with the large β-decay feeding of ^{72}Kr at excitation energies between 300 and 600 keV since the energy coming from the annihilation of the positron (1022 keV) is added to that of the deexcitation cascade.

An independent measurement was carried out to measure the ^{72}Br decay with the aim of removing its contribution to the ^{72}Kr decay measurement. It was performed with different time cycles, 84–60–90 s, as collection-waiting-measuring times to maximize the amount of radiation from the ^{72}Br decay. The subtraction of this contribution was performed by normalizing the ^{72}Kr decay run with the ^{72}Br decay run in the energy region beyond $Q_{EC}(^{72}\text{Kr}) = 5127(10)$ keV [25], where only radiation from the ^{72}Br decay, $Q_{EC}(^{72}\text{Br}) = 8801(7)$ keV [25], is present. The normalization procedure for the first run of the ^{72}Kr measurement is shown in Fig. 4 as an

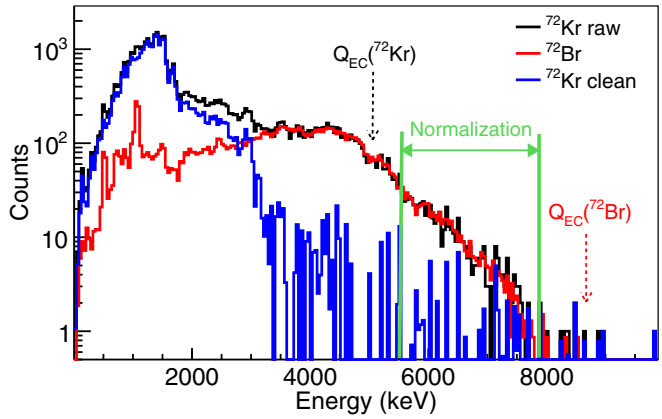

FIG. 4. (Color online) Comparison of the ^{72}Kr β-gated TAS spectrum (^{72}Kr raw), the ^{72}Br β-gated TAS spectrum (^{72}Br) measured independently and cleaned of ^{72,73}Se decay contaminations, and the resulting spectrum of the subtraction (^{72}Kr clean). The normalization of the spectrum corresponding to the decay of the daughter, ^{72}Br, with respect to the ^{72}Kr decay spectrum is done integrating over the energy interval indicated, where only counts from the contaminant must appear since it is beyond the $Q_{EC}(^{72}$Kr). After the subtraction, the statistics found in the ^{72}Kr clean spectrum beyond the $Q_{EC}(^{72}$Kr) energy fluctuates around the net zero value.

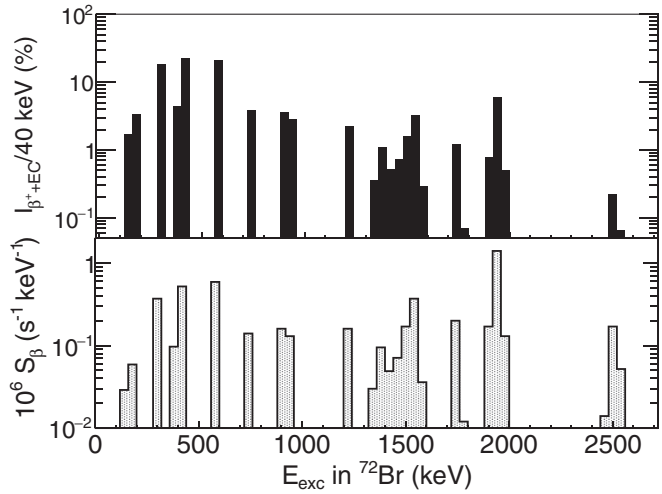

FIG. 5. Total $\beta^+ + \mathrm{EC}$ intensity distribution (upper panel) and β-decay strength distribution (lower panel) obtained in the analysis of the first set of data analyzed, "file 1" in Table I. Similar results were obtained for the other two spectra analysed. Both distributions are shown in 40-keV bins.

example. The spectrum of the ^{72}Br decay (red) is normalized to the spectrum taken for the ^{72}Kr decay (black) in order to perform the subtraction. The resulting spectrum (blue) is free of contamination and is the one used in the data analysis.

Unexpected contamination of ^{73}Se decay radiation from the $A = 73$ isobaric chain, see Fig. 1, was found in the ^{72}Br decay spectrum. The reason was the deposition of $A = 73$ beam outside the moving tape in the measurement performed just before. This contamination could be easily removed using an independently measured spectrum. Regarding the possible electronic pile-up of signals, looking at the ^{72}Br and ^{72}Kr spectra one observes that no counts are present beyond the corresponding Q_{EC} values of each decay. This tells us that the pile-up contribution is negligible. This component depends on the counting rate in the TAS detector, which was kept permanently at low values (≈3.5 kHz) during all of the measurements. Thus, the pile-up subtraction was not needed.

The procedure of subtraction of contaminants allowed us to obtain the clean ^{72}Kr decay spectrum needed for the analysis. At this stage, the analysis algorithm explained earlier, and in detail in Ref. [26], was applied to obtain the results presented in the next section.

IV. RESULTS AND DISCUSSION

A. Experimental results

The direct result from the β-gated data analysis is the β^+ feeding, I_{β^+}, which is extracted in a $\Delta E = 40$ keV width interval distribution due to the discretization of the response matrix. It extends up to 2680 keV excitation energy in ^{72}Br due to an upper limit imposed in the analysis. This limit was established to avoid the undesirable statistical fluctuations around a net zero value emerging in the spectrum after the contaminant subtraction. The average statistics in the energy region of the spectrum corresponding to excitation energies in ^{72}Br from 2680 keV up to the $Q_{\beta^+} = 4105$ keV averaged to zero. For this reason, we assumed in the present analysis that the unobserved β^+ feeding above the excitation energy of the upper limit is negligible and, therefore, the feeding observed is normalized to 100%.

The total $\beta^+ + \mathrm{EC}$ intensity, $I_{\beta^+ + EC}$, was obtained from the I_{β^+} using the tabulated EC/β^+ ratios [35]. The result is normalized to 100%, and the resulting β intensity distribution is shown in the upper panel of Fig. 5. The β-decay strength, S_β, is obtained using the expression

$$S_\beta(E_x) = \frac{I_{\beta^+ + EC}(E_x)}{f(Q_{EC} - E_x) \times T_{1/2} \times \Delta E}, \qquad (2)$$

where $I_{\beta^+ + EC}(E_x)$ is the total feeding ($\beta^+ + \mathrm{EC}$) for the levels included in a bin of ΔE width (chosen as 40 keV) which reaches up to E_x excitation energy, $f(Q_{EC} - E_x)$ is the value of the Fermi integral for a level located at E_x excitation energy, and $T_{1/2} = 17.1(2)$ s is the half-life of ^{72}Kr [23]. The value for the Fermi integral is taken from the tabulation given in [35]. The result for S_β is shown in the lower panel of Fig. 5.

The B(GT) is obtained from S_β using the expression

$$B(\mathrm{GT})(E_x) = \left(K \frac{g_V^2}{g_A^2}\right) \times S_\beta(E_x), \qquad (3)$$

where $K = 6143.6(17)$ s [36] and $\frac{g_A}{g_V} = -1.2695(29)$ [37]. In this way, the B(GT) has been obtained in a 40-keV binned distribution. For the comparison of our results with theoretical models, the B(GT) has been represented in such a way that every 40-keV bin contains the accumulated B(GT) from zero up to the energy corresponding to that bin. For this reason, all the results from our work are presented in terms of accumulated B(GT) distributions.

One important point to be considered is the direct ground state feeding. In the previous high-resolution spectroscopy work of Piqueras *et al.* [31] they found a ground state feeding of 35(1)% and an upper limit of 1.53% on the feeding to the isomeric state located at 101.3(3) keV [$T_{1/2} = 10.6(3)$ s]. Previous high-resolution studies provided inconsistent values of the ground state feeding ranging from 54% in [38] to 2(11)% in [39]. At this point it is worth noting that our analysis has a reduced sensitivity to the feeding to these two states. In both cases the TAS response is mainly to the emitted positron since no γ ray is emitted when feeding the ground state, and the probability to detect the 101.3 keV γ ray in coincidence with the β particle is almost negligible ($\sim 10^{-7}$) when the isomeric state is fed. Therefore, only the Bremsstrahlung radiation and the 511 keV γ rays coming from the positron annihilation can be observed in our TAS spectra in those cases. Our study suggests that the feeding to the ground and isomeric states is negligible. We can place an upper limit of 5% on the total feeding to both states. Our result is in agreement with that of Davids *et al.* [39], whose results are consistent with no feeding to the ground state.

B. Quality and stability checks

Two tests were performed to examine the reliability of the resulting β feeding distribution. The first is the comparison of the experimental β-gated TAS spectrum, d_i in Eq. (1), with that obtained through the convolution of the resulting β feeding distribution with the response matrix of the detector. The latter term is usually referred to as the reconstructed TAS spectrum and corresponds to the second term of Eq. (1). This comparison is shown in Fig. 6. We can see that the agreement is quite good for the whole spectrum, showing larger relative disagreement in the region with less statistics.

The second test is shown in Fig. 7 and consists of the comparison of the measured γ-transition intensities, I_γ, in the HPGe coaxial detector for the most intense transitions reaching the ground state of ^{72}Br, with those calculated from intensity balance using the feeding distribution resulting from the analysis and the deexcitation branching ratios used for the

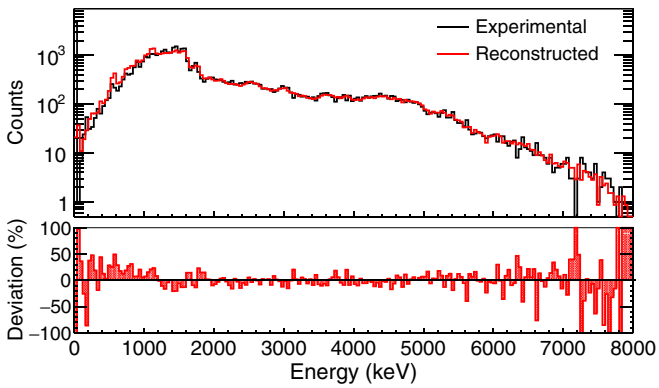

FIG. 6. (Color online) Comparison of the experimental and reconstructed β-gated TAS spectra of the first set of data taken for the ^{72}Kr decay measurement. Similar results are obtained for the other two spectra analyzed.

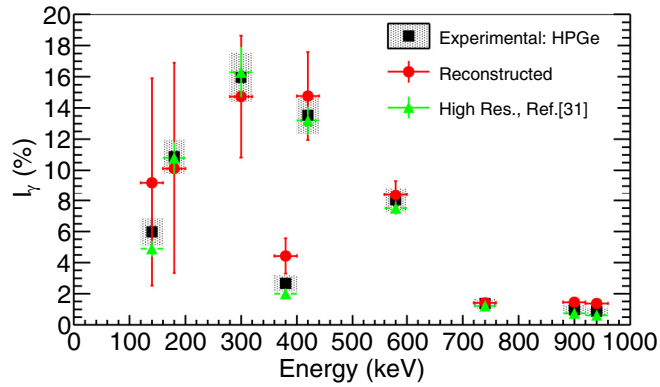

FIG. 7. (Color online) Comparison of the relative intensities of γ-transition following the ^{72}Kr β decay from our TAS analysis with those measured with the HPGe coaxial detector and the result from the high-resolution spectroscopy work of [31]. The comparison is made for the most intense transitions reaching the ^{72}Br ground state. The excitation energy of the deexciting state is indicated on the x axis in 40-keV intervals. The data correspond only to the first set of data and are normalized to the summed intensity (30.1% [31]) of transitions in the intervals (280–320) keV and (400–440) keV. Similar results were obtained for the other two sets of measurements.

levels. We note that the reproduction of this second observable is good as well. Altogether these tests indicate that the results discussed in the next section are reliable.

The resulting accumulated B(GT) distributions from the independent analyses of the three files measuring the ^{72}Kr decay are presented in Fig. 8. The distributions are compatible and, therefore, the final B(GT) distribution was estimated from the average of the three results. In the same way, the uncertainty has been estimated considering the dispersion between the results from the three analyses, the statistical uncertainty, as well as the uncertainty in the subtraction of the contaminants.

In addition, several tests on the stability of our results with respect to variations in the deexcitation scheme of the daughter

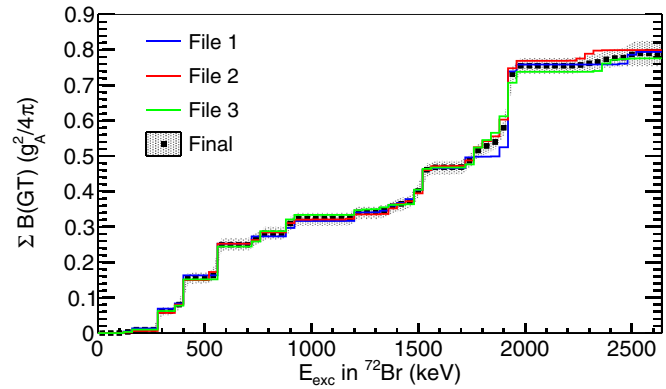

FIG. 8. (Color online) Comparison of the accumulated B(GT) distributions obtained in the analyses of the individual data files taken for the three measurements of the ^{72}Kr decay together with their average taken as the definitive result. The error bars were determined taking into account the statistical error, dispersion of the three results, and the uncertainty from the subtraction of the contaminants.

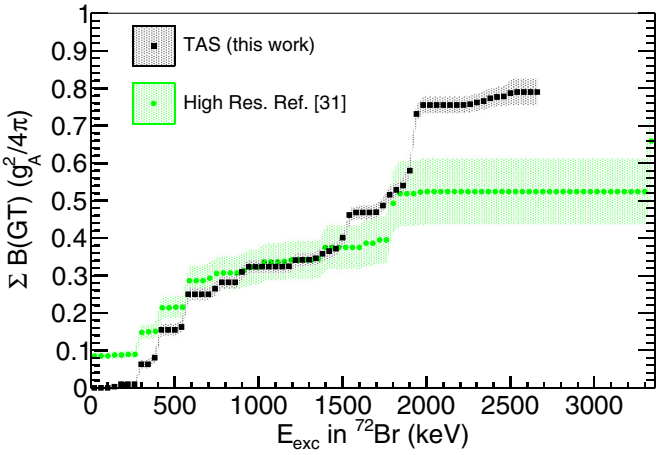

FIG. 9. (Color online) Comparison of the accumulated B(GT) distribution with results from the high-resolution spectroscopy study of Piqueras *et al.* [31]. Evidence of the Pandemonium effect can be seen.

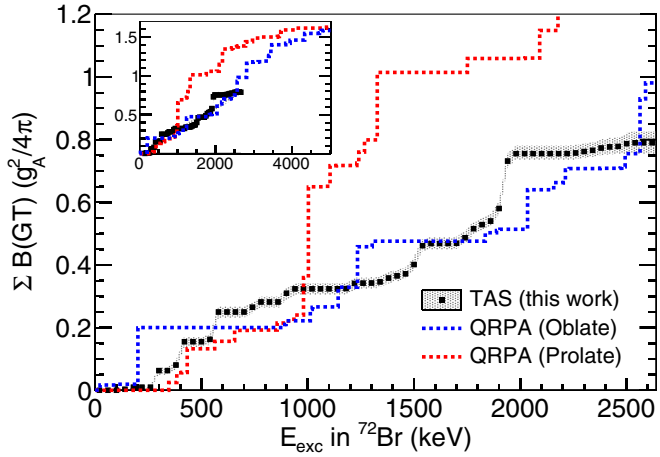

FIG. 10. (Color online) Comparison of the experimental accumulated $B(GT)$ distribution found in this work (black dots) with predictions from QRPA calculations using the SLy4 Skyrme interaction [40]. The inset shows the comparison in an extended energy region up to 5 MeV (see text for more details).

nucleus were presented in Ref. [30], where modifications of the known and unknown parts of the deexcitation scheme were introduced and no noticeable differences in the accumulated B(GT) distribution were found. This again supports the reliability of our results and stability with respect to the uncertainty arising from the limited knowledge of the level scheme of the daughter nucleus.

C. Comparison with high-resolution results

Figure 9 shows the accumulated B(GT) distribution obtained in our work and the result of the high-resolution spectroscopy study of Piqueras *et al.* [31], which is the most complete spectroscopic study of this decay carried out so far. Evidence of the Pandemonium effect can be observed since more strength is located at lower energies in the high-resolution study than in our TAS work, and a large amount of the B(GT) is missed in the high-resolution measurement from 1.5 MeV on, as expected. The influence of this effect is not as remarkable as in other studies, at least in the energy window explored in the present work. However, a TAS study to determine the strength for excitation energies above 2.7 MeV, ideally in the full Q_{EC} window (5.1 MeV), would be needed to elucidate how important this effect is in the decay of interest.

D. Comparison with predictions from theoretical calculations

Different theoretical approaches are available to describe the properties of nuclei in the A $\approx$ 70–80 region of the chart of nuclides. An appropriate way of comparing our results with predictions from these calculations is through the accumulated B(GT) distributions.

Deformed quasiparticle random phase approximation (QRPA) calculations, based on a Skyrme self-consistent mean field approach, were performed for nuclei in this mass region [6,40] and motivated the present work. The formalism is presented in detail in Refs. [6,40] and is only summarized briefly here. A deformed Hartree-Fock (HF) mean field is generated with Skyrme-type forces including pairing correlations in the BCS approximation. Afterwards, a constrained HF method is employed to analyze the energy surfaces and to find the HF energy minima at the corresponding nuclear deformations. The $B(GT)$ transition strengths are then determined for the various equilibrium deformations by solving the QRPA equations under the assumption that the parent ground state and the states fed in the daughter nucleus have the same deformation. A quenching factor of 0.77 is applied to take into account in an effective way all the correlations not properly included in this approach [41]. In this framework, two energy minima close in energy, one oblate and another prolate, were found for the ^{72}Kr case. Their corresponding B(GT) distributions obtained using the SLy4 Skyrme-type force [40] are shown together with our results in Fig. 10. SLy4 [42] is one of the most successful Skyrme interactions and has been widely used. The protocol used to fit the parameters of the force aims to improve the isotopic properties of finite nuclei away from the β-stability line.

The distributions obtained for the oblate and prolate deformations are remarkably different, as shown in Fig. 10. The one for the oblate deformed minimum is in rather good agreement with our experimental results. The prolate distribution reproduces the tendency of the data rather well up to an excitation energy of 1 MeV but for higher energies it predicts larger B(GT) values than are found experimentally. The total amount of B(GT) determined experimentally in the energy window studied, 0.79(4) $g_A^2/4\pi$, is close to that predicted for the oblate minimum, 0.98 $g_A^2/4\pi$, in contrast to the 1.4 $g_A^2/4\pi$ accumulated B(GT) predicted for the prolate shape; see Table II. This comparison suggests a dominant oblate deformation for the ^{72}Kr ground state, in good agreement with the conclusions of Ref. [11].

Shell-model calculations have been performed using a ^{56}Ni core including the orbits $1p_{3/2}$, $0f_{5/2}$, $1p_{1/2}$, $0g_{9/2}$, and $1d_{5/2}$ as valence space and the JUN45 effective interaction described

TABLE II. Accumulated B(GT) values (in units of $g_A^2/4\pi$) for the ^{72}Kr decay obtained in this work in comparison with theoretical predictions.

Energy (keV)	Expt. TAS	QRPA [40]		EXVAM [19]		Shell model
		Obl.	Pro.	Bonn-A	Bonn-CD	
120	0.0(0)	0.019	0	0.03	0.06	0.13
1000	0.32(2)	0.22	0.36	0.12	0.17	0.24
2000	0.76(2)	0.51	1.10	0.55	0.51	0.64
2680	0.79(4)	0.98	1.40	0.63	0.59	0.87
5000		1.58	1.64	0.82	0.70	1.23

in Ref. [43]. As in the QRPA approach, a standard quenching factor of 0.77 [41] was applied. In this calculation, the resulting ground state can be interpreted as a mixed configuration of oblate and prolate states in approximately similar proportions. The oblate state belongs to a band whose corresponding deformation parameter is $\beta_2 = -0.3$ and the prolate state to one with $\beta_2 = 0.4$. The comparison of the predictions from this approach with our results is shown in Fig. 11. They reproduce the experimental distribution in the whole energy range, except at low energy where the model predicts some ground state strength not observed experimentally. Instead, this strength is found to the levels at 310 and 415 keV excitation energy. The accumulated B(GT) predicted up to 2.7 MeV, 0.87 $g_A^2/4\pi$, is not far from the experimental value in the energy window studied, 0.79(4) $g_A^2/4\pi$, if one considers the error bars, as shown in Table II.

The complex excited VAMPIR beyond-mean-field variational approach (EXVAM) was already applied to study the ^{72}Kr decay [19]. These calculations were employed for the description of the shape coexistence phenomena in $A \approx 100$ [44] including Gamow-Teller strength distributions [45]. The results for the strength obtained using the Bonn-A and Bonn-CD interactions taken from [19] are shown in Table II in comparison with our data. Their predictions were already compared in [19] with the B(GT) distribution obtained from the high-resolution study of Piqueras *et al.* [31] with a remarkably good agreement. However, the results presented here show a larger amount of strength than [31] in the energy region 2.0–2.7 MeV, as can be seen in Fig. 9 and Table II. Therefore, the reproduction of the TAS data is not as satisfactory as it was for the high-resolution results, but still the calculations follow the trend. One has to keep in mind, as stated in [19], that predictions could be modified, especially in the high-energy region, by including higher lying configurations and changes in the renormalization of the effective interaction. The calculated wave functions for the parent ground state in this approach indicates strong oblate-prolate shape mixing, with oblate/prolate mixing amplitudes of 64%/29% using the Bonn A interaction and 50%/38% using the Bonn CD interaction. This interpretation is in agreement with the shell model calculations presented for the first time in this work.

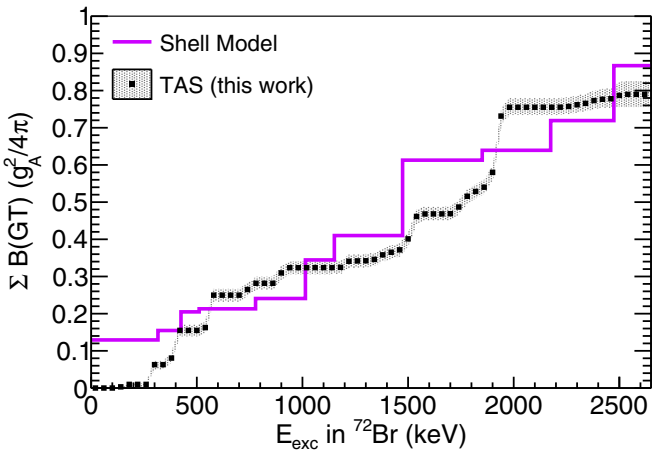

FIG. 11. (Color online) Comparison of the experimental accumulated $B(GT)$ distribution found in this work (black dots) with predictions from shell-model calculations.

E. Discussion

The experimental B(GT) distribution obtained from the present TAS study has been compared to predictions from QRPA [40], shell-model calculations here presented for the first time, and EXVAM variational calculations [19]. The comparison with QRPA calculations [40] suggests a dominantly oblate deformation for the ^{72}Kr ground state. However, shell-model and EXVAM variational calculations describe rather well the B(GT) distribution in the energy window studied, and they agree in pointing towards a mixing between oblate and prolate configurations in approximately equal proportions for the ground state.

Previous experimental evidence [11,13,14] seems to indicate a predominant oblate deformation. The large $B(E2; 4^+ \rightarrow 2^+)$ value and the $B(E2; 2^+ \rightarrow 0_1^+)$ value lower than expected [14] suggest the occurrence of a rapid prolate-oblate shape transition from the purely prolate band identified in [12] towards the ground state. Although suggesting a dominant oblate deformation for the ground state, a certain amount of mixing with the prolate deformed 0^+ state was suggested by another experimental work [11]. The energy of the first excited 0^+ state, determined in that work at 671(2) keV, indicated a mixing amplitude of 10% with the 0^+ oblate ground state from a two-level mixing model.

The good match between the experimental B(GT) distribution found in this work with the one predicted for an oblate deformed ^{72}Kr ground state in the QRPA calculations, see Fig. 10, supports either a pure oblate deformation or a rather small degree of mixing with the prolate 0_2^+ state. This is in agreement with the 10% previously reported in [11]. Despite this similarity, we cannot exclude the possibility of a sizable shape mixing as indicated by shell-model and EXVAM calculations. One has to keep in mind that the QRPA approach presented here only calculates the B(GT) distributions for states with pure oblate or prolate deformation, which are the minima found in the energy surface for the nucleus of interest. Furthermore, the transitions considered in the calculations are those connecting states with the same deformation in parent and daughter nuclei. Therefore, a firm statement on the oblate

or shape mixing for the deformation of the ^{72}Kr ground state cannot be made at this stage.

It is worth noting that the shell-model and QRPA approaches predict different values for the accumulated B(GT) up to the Q_{EC} value of 5127(10) keV for the ^{72}Kr decay (see Table II). Our analysis shows negligible β^+ feeding to levels above 2.7 MeV. Both experiment and the shell model show a much reduced rate of increase in the accumulated B(GT) beyond 2.7 MeV.

V. SUMMARY AND CONCLUSIONS

The total absorption spectroscopy technique has been applied to study the ^{72}Kr β decay. The accumulated B(GT) is extracted in a 40-keV binned distribution up to an excitation energy of 2.7 MeV with a total value of 0.79(4) $g_A^2/4\pi$. This distribution is compared with predictions from the best performing theoretical models in the mass region. The comparison with deformed Skyrme HF+BCS+QRPA calculations indicates a dominant oblate deformation for the ^{72}Kr ground state. The same interpretation has been obtained from the $B(E2)$ values for the $4^+ \rightarrow 2^+$ and $2^+ \rightarrow 0_1^+$ transitions [14]. Shell-model calculations performed in this mass region for the first time reproduce very nicely the experimental data. They describe the ground state of ^{72}Kr as a mixture of oblate and prolate configurations in similar proportions. A larger mixing amplitude in the ground state than the 10% previously proposed [11] is suggested by our shell-model calculations. The EXVAM calculations [19] arrive at similar conclusions.

Summarizing, although the results of our β-decay study suggest that the ^{72}Kr ground state is predominantly oblate deformed in the framework of the QRPA calculations, mixing with prolate deformed configurations cannot be excluded as shown by shell-model and EXVAM calculations. It was one of the goals of this work to compare the measured and calculated $B(GT)$ distributions for the decay of ^{72}Kr in order to infer its deformation. However ^{72}Kr is a particularly delicate case for two reasons: first because it is an $N = Z$ nucleus, and second because there is shape coexistence at very low excitation energy and even shape mixing in the ground state is plausible. These facts make the calculations very sensitive to small changes in the parameters, and the results are not as robust as in the cases studied earlier. A new measurement of this decay over the full energy window could shed light on the deformation of the ground state of ^{72}Kr as the theoretical models predict different values of the accumulated B(GT) at high excitation energy.

In conclusion, it is very clear that two shapes, oblate and prolate, coexist in ^{72}Kr with rotational bands of different character built on them. However whether the 0_1^+ ground state and the first excited 0_2^+ state are two states with different deformations or whether they are both mixed still remains an open question.

ACKNOWLEDGMENTS

The authors thank A. Petrovici for useful discussions. J.A.B. acknowledges the predoctoral grant BES-2008-009412 associated with the research project FPA2007-62170 funded by Ministerio de Ciencia e Innovación (Spain). This work has been partly supported by the Spanish Ministerio de Economía y Competitividad (MINECO) through projects FPA2012-32443, FPA2011-24553, FPA2011-29854-C04-01, FPA2013-41267-P, FPA2014-52823-C2-1-P and FIS2011-23565, by STFC-UK (Grant No. ST/F012012/1) and by the European Union by means of the European Commission within its Seventh Framework Programme (FP7) via ENSAR (Contract No. 262010).

[1] W. Nazarewicz, J. Dudek, R. Bengtsson, T. Bengtsson, and I. Ragnarsson, Nucl. Phys. A **435**, 397 (1985).
[2] P. Moller, J. R. Nix, W. D. Myers, and W. J. Swiatecki, At. Data Nucl. Data Tables **59**, 185 (1995).
[3] S. G. Nilsson, Mat. Fys. Medd. K. Dan. Vidensk. Selsk. **29**, 16 (1955).
[4] E. Nácher *et al.*, Phys. Rev. Lett. **92**, 232501 (2004).
[5] C. J. Lister, P. J. Ennis, A. A. Chishti, B. J. Varley, W. Gelletly, H. G. Price, and A. N. James, Phys. Rev. C **42**, R1191 (1990).
[6] P. Sarriguren, E. Moya de Guerra, and A. Escuderos, Nucl. Phys. A **658**, 13 (1999); **691**, 631 (2001).
[7] P. Moller, A. J. Sierk, R. Bengtsson, H. Sagawa, and T. Ichikawa, Phys. Rev. Lett. **103**, 212501 (2009).
[8] J. H. Hamilton *et al.*, Phys. Rev. Lett. **32**, 239 (1974).
[9] R. B. Piercey *et al.*, Phys. Rev. Lett. **47**, 1514 (1981).
[10] B. J. Varley, M. Campbell, A. A. Chishti, W. Gelletly, L. Goettig, C. J. Lister, A. N. James, and O. Skeppstedt, Phys. Lett. B **194**, 463 (1987).
[11] E. Bouchez *et al.*, Phys. Rev. Lett. **90**, 082502 (2003).
[12] G. de Angelis *et al.*, Phys. Lett. B **415**, 217 (1997).
[13] A. Gade *et al.*, Phys. Rev. Lett. **95**, 022502 (2005); **96**, 189901 (2006).
[14] H. Iwasaki *et al.*, Phys. Rev. Lett. **112**, 142502 (2014).
[15] B. S. Nara Singh (private communication).
[16] I. Hamamoto and X. Z. Zhang, Z. Phys A **353**, 145 (1995).
[17] C. L. Duke, P. G. Hansen, O. B. Nielsen, G. Rudstam, and ISOLDE Collaboration (CERN), Nucl. Phys. A **151**, 609 (1970).
[18] J. C. Hardy, L. C. Carraz, B. Jonson, and P. G. Hansen, Phys. Lett. B **71**, 307 (1977).
[19] A. Petrovici, K. W. Schmid, O. Radu, and A. Faessler, Phys. Rev. C **78**, 044315 (2008).
[20] A. B. Pérez-Cerdán *et al.*, Phys. Rev. C **88**, 014324 (2013).
[21] E. Poirier *et al.*, Phys. Rev. C **69**, 034307 (2004).
[22] Isotope mass separator on-line facility (ISOLDE), http://isolde.web.cern.ch.
[23] D. Abriola, Nucl. Data Sheets **111**, 1 (2010).
[24] R. B. Firestone, *Table of Isotopes*, 8th ed. (Wiley Interscience, New York, 1996).
[25] M. Wang, G. Audi, A. H. Wapstra, F. G. Kondev, M. MacCormick, X. Xu, and B. Pfeiffer, Chin. Phys. C **36**, 1603 (2012).
[26] J. L. Taín and D. Cano-Ott, Nucl. Instrum. Methods A **571**, 728 (2007).
[27] J. L. Taín and D. Cano-Ott, Nucl. Instrum. Methods A **571**, 719 (2007).

[28] D. Cano-Ott, J. L. Taín, A. Gadea, B. Rubio, L. Batist, M. Karny, and E. Roeckl, Nucl. Instrum. Methods A **430**, 333 (1999).
[29] GEANT4-CERN international collaboration, http://geant4.cern.ch/.
[30] J. A. Briz *et al.*, in *Proceedings of the Conference on Advances in Radioactive Isotope Science (ARIS2014)*, edited by J. Zenihiro, JPS Conf. Proc. No. 6 (JPS, Tokyo, 2015), p. 020050.
[31] I. Piqueras *et al.*, Eur. Phys. J. A **16**, 313 (2003).
[32] J. A. Briz *et al.*, in *Proceedings of La Rábida 2009, International Scientific Meeting on Nuclear Physics: Basic Concepts in Nuclear Physics: Theory, Experiments and Applications*, edited by J. A. Caballero, C. E. Alonso, M. V. Andrés, J. E. García Ramos, and F. Pérez-Bernal, AIP Conf. Proc. No. 1231 (AIP, New York, 2012), p. 203.
[33] W. Dilg, W. Schantl, H. Vonach, and M. Uhl, Nucl. Phys. A **217**, 269 (1973).
[34] G. A. Bartholomew, E. D. Earle, A. J. Ferguson, J. W. Knowles, and M. A. Lone, in *Advances in Nuclear Physics*, edited by M. Baranger and E. Vogt (Springer US, New York, 1973), Vol. 7, pp. 229–324.
[35] N. B. Gove and M. J. Martin, Nucl. Data Tables **10**, 205 (1971).
[36] J. C. Hardy and I. S. Towner, Phys. Rev. C **79**, 055502 (2009).
[37] J. C. Hardy and I. S. Towner, Nucl. Phys. News **16**, 11 (2006).
[38] H. Schmeing, J. C. Hardy, R. L. Graham, J. S. Geiger, and K. P. Jackson, Phys. Lett. B **44**, 449 (1973).
[39] C. N. Davids and D. R. Goosman, Phys. Rev. C **8**, 1029 (1973).
[40] P. Sarriguren, Phys. Rev. C **79**, 044315 (2009).
[41] G. F. Bertsch and I. Hamamoto, Phys. Rev. C **26**, 1323 (1982).
[42] E. Chabanat, P. Bonche, P. Haensel, J. Meyer, and R. Schaeffer, Nucl. Phys. A **635**, 231 (1998).
[43] M. Honma, T. Otsuka, T. Mizusaki, and M. Hjorth-Jensen, Phys. Rev. C **80**, 064323 (2009).
[44] A. Petrovici, Phys. Rev. C **85**, 034337 (2012).
[45] D. Jordan *et al.*, Phys. Rev. C **87**, 044318 (2013).